Hindawi Publishing Corporation
Advances in Condensed Matter Physics
Volume 2014, Article ID 232510, 8 pages
http://dx.doi.org/10.1155/2014/232510

Research Article

Study on Macroscopic and Microscopic Mechanical Behavior of Magnetorheological Elastomers by Representative Volume Element Approach

Shulei Sun,[1] Xiongqi Peng,[2] and Zaoyang Guo[3]

[1] *School of Mechanical Engineering, Northwestern Polytechnical University, Xi'an 710072, China*
[2] *School of Materials Science and Engineering, Shanghai Jiaotong University, Shanghai 200030, China*
[3] *Department of Engineering Mechanics, Chongqing University, Chongqing 400044, China*

Correspondence should be addressed to Xiongqi Peng; xqpeng@sjtu.edu.cn and Zaoyang Guo; zyguo01@gmail.com

Received 20 December 2013; Revised 5 June 2014; Accepted 5 June 2014; Published 10 July 2014

Academic Editor: Daniel Balint

By using a representative volume element (RVE) approach, this paper investigates the effective mechanical properties of anisotropic magnetorheological elastomers (MREs) in which particles are aligned and form chain-like structure under magnetic field during curing. Firstly, a three-dimensional RVE in zero magnetic field is presented in ABAQUS/Standard to calculate the macroscopic mechanical properties of MREs. It is shown that the initial shear modulus of MREs increases by 56% with a 20% volume fraction of particles compared to that of pure rubber. Then by introducing the Maxwell stress tensor, a two-dimensional plane stress RVE for the MRE is developed in COMSOL Multiphysics to study its response under a magnetic field. The influences of magnetic field intensity, radius of particles, and distance between two adjacent particles on the macroscopic mechanical properties of MRE are also investigated. The results show that the shear modulus increases with the increase of the applied magnetic field intensity and the radius of particles and the decrease of the distance between two adjacent particles in a chain. The predicted numerical results are consistent with theoretical results from Mori-Tanaka model, double inclusion model, and dipole model.

1. Introduction

Increasing interest in magnetorheological elastomers (MREs), in which micron sized ferrous particles are dispersed in soft matrix such as rubber, is driven by their unique property of magnetic-mechanical coupling [1–4]. This kind of material renders changeable shear modulus with various applied magnetic field. MREs have many advantages such as good stability, controllability, reversibility, and fast responsiveness and are thus widely applied in variable stiffness devices. In recent years, many researchers have focused on MREs. Gong et al. [5–8] carried out an investigation on preparation and application of MREs. Dorfmann and Ogden [9] developed constitutive models for MREs under finite deformation. Besides, theoretical dipole model, which takes into account the magnetic dipole interaction between two adjacent particles in a chain, was widely used to study the mechanical properties of MREs [10–13]. Because of the complexity involved in magnetic-mechanical coupling, few studies on the macro-/microscopic mechanical properties of MREs were carried out based on finite element method (FEM).

In order to study the unique response of anisotropic MREs, the property of a field under localized and microscopic condition has to be homogenized to get macroequivalent properties. Therefore, both macro- and microscales should be considered. This paper aims to study the effective mechanical properties of anisotropic MREs by using FEM. A three-dimensional representative volume element (RVE) with microscale for the MRE is developed in ABAQUS/Standard and solved by assigning periodic boundary conditions to obtain its macroscopic mechanical properties with no field applied. Secondly, by introducing the Maxwell stress tensor, a two-dimensional plane stress RVE for the MRE is developed in COMSOL Multiphysics to study its response under a magnetic field. Finally, influences of magnetic field intensity,

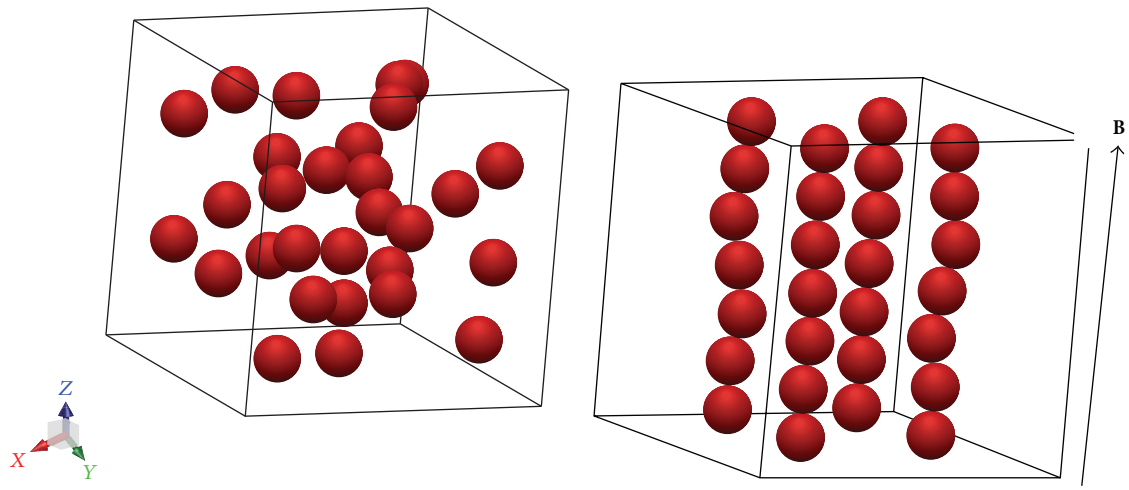

(a) Isotropic MREs (b) Anisotropic MREs

Figure 1: Sketches of MREs.

radius of particles, and distance between two adjacent particles in a chain on the macroscopic mechanical properties of MRE are also investigated.

2. Basics of MRE Composites with Periodic Structures

2.1. Microstructure of MREs. MREs consist of micron sized silicon rubber matrix and magnetizable carbonyl sphere particles (about 3 to 5 μm). They are classified into two parts: isotropic MREs (Figure 1(a)) and anisotropic MREs (Figure 1(b)).

2.2. Governing Equations. Several methods can be used to compute the magnetic force, for example, the Lorentz, the Maxwell stress tensor, and the virtual work method [14]. For numerical simulation without electric current, the Maxwell stress tensor is a mature way and is widely used [15–18]. Cauchy's equation of continuum mechanics reads

$$\rho \frac{d^2\mathbf{r}}{dt^2} = \nabla \cdot \mathbf{T} + \mathbf{f}_{\text{ext}}, \tag{1}$$

where ρ is density and $\mathbf{r}$ is the coordinates of a material point, $\mathbf{T}$ is the stress tensor, and $\mathbf{f}_{\text{ext}}$ is an external volume force such as gravity ($\mathbf{f}_{\text{ext}} = \rho\mathbf{g}$). In the stationary case, there is no acceleration, and the equation representing the force balance is

$$\mathbf{0} = \nabla \cdot \mathbf{T} + \mathbf{f}_{\text{ext}}. \tag{2}$$

In certain cases, the stress tensor $\mathbf{T}$ can be divided into two parts. One depends on the electromagnetic field and the other is the mechanical stress tensor:

$$\mathbf{T} = \mathbf{T}_{\text{EM}} + \boldsymbol{\sigma}_M. \tag{3}$$

It is sometimes convenient to use a volume force instead of the stress tensor for the electromagnetic induced stress tensor $\mathbf{T}_{\text{EM}}$:

$$\mathbf{f}_{\text{em}} = \nabla \cdot \mathbf{T}_{\text{EM}}. \tag{4}$$

Then (2) can be rewritten as

$$\mathbf{0} = \nabla \cdot \boldsymbol{\sigma}_M + \mathbf{f}_{\text{em}} + \mathbf{f}_{\text{ext}}. \tag{5}$$

The expressions for the stress tensor in a general electromagnetic context stem from a fusion of material theory, thermodynamics, continuum mechanics, and electromagnetic field theory. With the introduction of thermodynamic potentials of mechanical, thermal, and electromagnetic effects, explicit expressions for the stress tensor can be derived in a convenient way by forming the formal derivatives with respect to different physical fields [19, 20]. Alternative derivations can be made for a vacuum [21]. But it is difficult to polarize and magnetize materials. In general, an elastic solid material of that is dielectric and magnetic (nonzero $\mathbf{M}$). The stress tensor is given as

$$\mathbf{T}_{\text{EM}} = \frac{1}{\mu_0}\mathbf{B} \cdot \mathbf{B}^T - \mathbf{M}\mathbf{B}^T - \frac{1}{2\mu_0}(\mathbf{B} \cdot \mathbf{B} - \mathbf{M} \cdot \mathbf{B})\,\mathbf{I}, \tag{6}$$

where $\mathbf{B}$ is the magnetic flux density, $\mathbf{M}$ is the magnetization vector, $\mathbf{I}$ is the identity matrix, and μ_0 is the magnetic permeability of vacuum, which is $4\pi \times 10^{-7}$ H/m. Thus the Maxwell stress tensor can be applied on the boundary of iron particles to obtain the coupling of stress and magnetic field.

2.3. Representative Volume Element and Periodic Boundary Conditions. In the theory of composite materials, representative volume element (RVE) is the smallest volume over which a measurement can be made that will yield a value representing the whole. Periodic boundary conditions (PBC) are often used to simulate a large system by modeling a small part that is far from its edge. Many researchers [22–24]

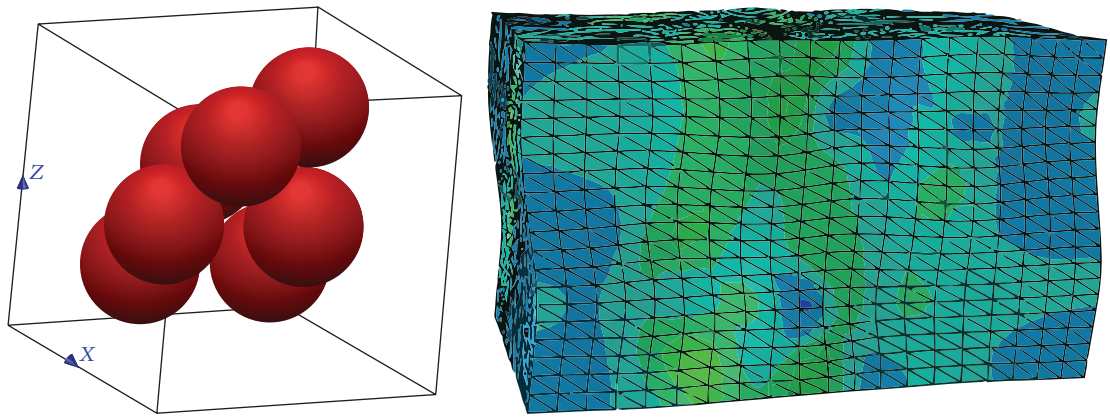

(a) RVE of MREs (b) Tension deformation of MREs

Figure 2: Several particles of orthotropic MREs.

studied PBC and proved that PBC ensure the continuity of the deformation field. Because PBC will be applied to RVE models in FEM simulations, it is also required that RVE models have periodic microstructures. That is, if a particle intersects the RVE surface, it must be split into an appropriate number of parts and copied to the opposite sides. The interface between every two adjacent RVEs must have the same displacement and stress field, that is, satisfying the continuity conditions of stress. For a given average deformation gradient $\overline{\mathbf{F}}$ applied to the RVE model, the PBC can be represented by the following general format [25]:

$$\mathbf{x}(Q_1) - \mathbf{x}(Q_2) - \left(\overline{\mathbf{F}} - \mathbf{I}\right)\left[\mathbf{X}(Q_1) - \mathbf{X}(Q_2)\right] = \mathbf{0}, \quad (7)$$

$$\mathbf{V}(Q_1) = -\mathbf{V}(Q_2), \quad (8)$$

where Q_1 and Q_2 are the nodes of the opposite adjacent faces, $\mathbf{I}$ is the identity matrix, $\mathbf{V}$ is the force applied on the node, and $\mathbf{X}$ and $\mathbf{x}$ denote the position vectors of a material point in the original (undeformed) and deformed configuration, respectively. When the opposite faces are parallel, from (7), $(\overline{\mathbf{F}} - \mathbf{I})[\mathbf{X}(Q_1) - \mathbf{X}(Q_2)]$ is a constant. We can use an equation constraint to realize (7) in FEA software. It can be proved that when (7) is satisfied, then (8) is also satisfied. If (7) and (8) are contented, the average mechanical properties from the RVE are those of the whole MREs.

2.4. Approaches for Macromechanical Property Prediction. There are two ways to get the macromechanical properties of composites. One is the direct FEM; the other is mean field homogenization. FEM is based on a RVE and gives accurate and detailed microfield. The second approach is based on the theory of Eshelby inclusion of various approximate models [26], such as the self-consistent model, generalized self-consistent model, Mori-Tanaka model [27], and double inclusions model [28]. It only gives approximations to the volume averages of stresses and strains, either at the macrolevel or in each phase. With the development of FEM, the first approach is widely used [29, 30] and can get accurate results than the second way. In this paper, the Mori-Tanaka model and double inclusion model in the absence of an effective magnetic field are used and compared with the FEM. In the case of a magnetic field, numerical FEM simulation based on the RVE is selected.

3. Material Description of the MRE

3.1. Carbonyl Iron Particles. Particulate filler herein is carbonyl iron particle, which is a typical high permeability material having low remanence and high magnetic saturation rate. The material parameters are given as follows: Young's modulus is 210 GPa, Poisson's ratio is 0.33 [31], and shear modulus is 78.94 GPa. The relative magnetic permeability is assumed to be 100.

3.2. Mechanical Properties of Rubber Matrix. The silicon rubber used as matrix in MREs can be modeled by a form of free energy function of Mooney-Rivlin [32], which is suitable for moderate finite deformation:

$$W = C_{10}\left(\bar{I}_1 - 3\right) + C_{01}\left(\bar{I}_2 - 3\right) + \frac{\kappa}{2}(J-1)^2, \quad (9)$$

where $\bar{I}_1$ and $\bar{I}_2$ are the modified invariants, J is the ratio of the deformed elastic volume, and κ is the bulk modulus. The parameters C_{10} and C_{01} are 0.4 MPa and 0.1 MPa, respectively. The initial shear modulus of the silicon rubber can be calculated from $G = 2(C_{10} + C_{01})$ as 1 MPa [33]. It is assumed that Poisson's ratio ν is 0.47 for small compressibility. The relative magnetic permeability of silicon rubber is assumed to be 1. The bulk modulus κ and the initial Young modulus E can be calculated from the following equation as $\kappa = 16.33$ MPa, $E = 2.94$ MPa:

$$\kappa = \frac{2G(1+\nu)}{3(1-2\nu)}, \qquad E = 2G(1+\nu). \quad (10)$$

4. Macro-/Micromechanical Properties of the Isotropic MRE without Magnetic Field

As shown in Figure 2(a), numerical model of a three-dimensional RVE for the isotropic MRE is implemented

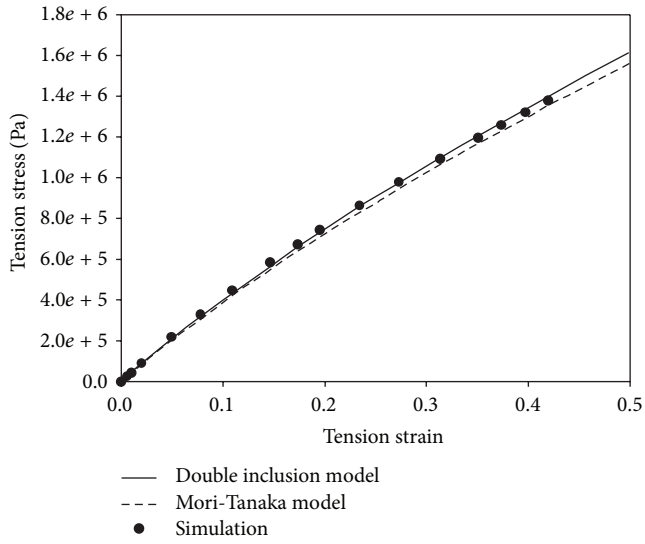

Figure 3: Stress-strain curve without a magnetic field.

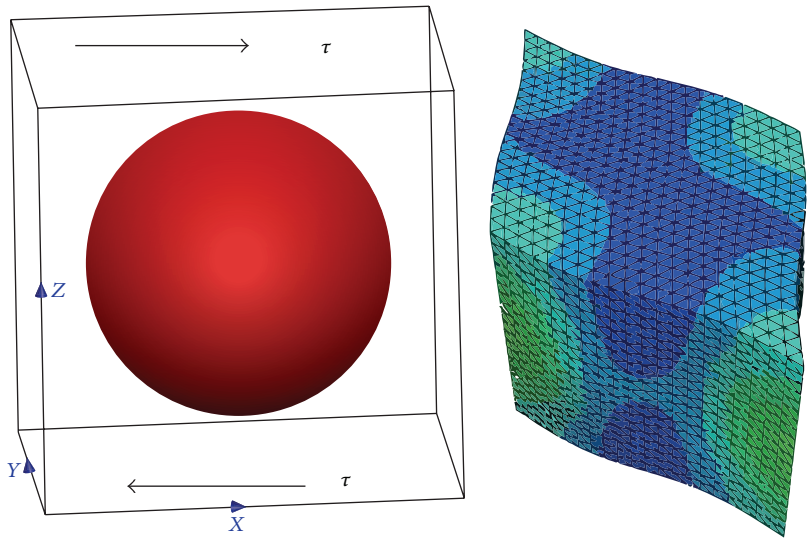

(a) RVE of the orthotropic MRE

(b) Deformation of the orthotropic MRE

Figure 4: Orthotropic MREs.

in ABQAUS/Standard and a tension deformation is applied without a magnetic field. The volume fraction of particles is 0.2. The deformation of RVE with applied periodic boundary condition is shown in Figure 2(b).

Figure 3 shows the macroscopic tension stress-strain curve of the orthotropic MRE. As can be seen from Figure 3, the stress-strain response of the MRE is nonlinear. The numerical results are consistent with the predictions computed by the double inclusion model and Mori-Tanaka model. It can be obtained from Figure 3 that the initial Young modulus is 4.16 MPa.

Then a RVE with zero magnetic field which has one particle with a volume fraction of 0.2 is established. As can be seen from Figure 4, periodic boundary condition and shear strain are applied on the RVE. The predicted shear stress-strain curve is presented in Figure 6. It can be calculated from Figure 5 that the initial shear modulus is 1.56 MPa.

5. Macro-/Micromechanical Properties of Anisotropic MRE with Magnetic Field

5.1. Dipole Models. In the dipole model, the free energy function in MREs can be decomposed into three parts nominally representing the energy contributions from the matrix, particle, and the coupled interaction of magnetic filed and particles. The magnetic dipolar interaction between adjacent particles in a chain is illustrated in Figure 6.

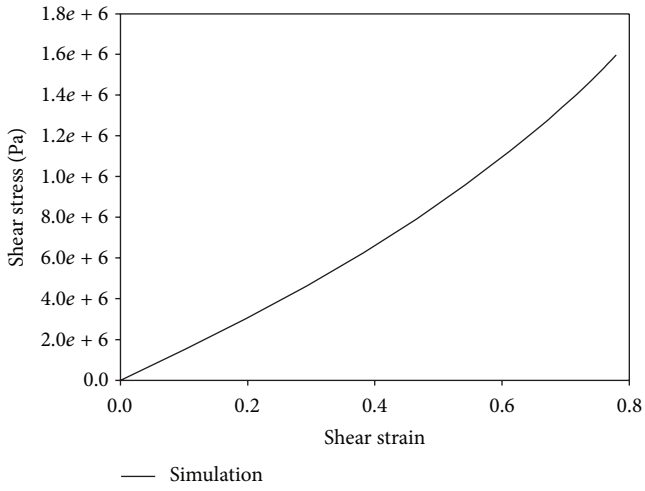

FIGURE 5: Shear stress-strain curve without a magnetic field in the orthotropic MRE.

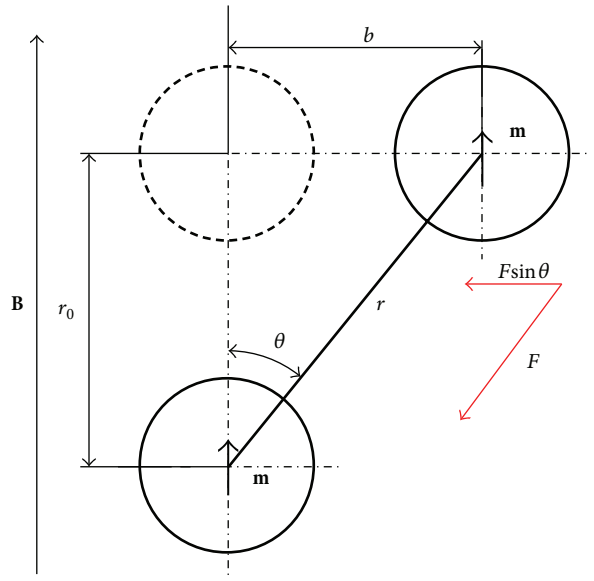

FIGURE 6: Dipole interaction in a straight chain.

The dipole model assumes that the interaction energy of the two dipoles is [34]

$$W = \frac{\mathbf{m}^2}{4\pi\mu_0\mu_1 r^3}\left(1 - 3\cos^2\theta\right), \tag{11}$$

where μ_0 is the vacuum permeability, μ_1 is the relative permeability, and $\mathbf{m}$ is the magnetic dipole moment. It is assumed that per unit volume has N pieces of particles, so $N = 6\phi/\pi d^3$ where d is the diameter of a particle and ϕ is the volume fraction of particles. It is defined that the shear strain is $\gamma = b/r_0$ and the magnetic energy (per unit volume) is

$$W = \frac{3\phi\left(\lambda^2 - 1\right)\mathbf{m}^2}{2\pi^2\mu_0\mu_1 d^3 r_0^3(1+\lambda^2)^{5/2}}. \tag{12}$$

The initial shear modulus can be obtained by the second differentiation of W with respect to λ. When λ approaches zero, the contribution to the shear stiffness can be written as

$$G = \left.\frac{\partial^2 W}{\partial\gamma^2}\right|_{\gamma\to 0} = \frac{\phi\mathbf{m}^2 d^3}{2\mu_0\mu_1 r_0^3}. \tag{13}$$

As is indicated in (13), the magnetic field strength and diameter of particles and the distance between two adjacent particles in a chain are key factors affecting the initial shear modulus.

5.2. Magnetic Equations. In a current free region, where $\nabla \times \mathbf{H} = 0$ and $\mathbf{H}$ is magnetic field strength, it is possible to define a scalar magnetic potential V_m from the relation $\mathbf{H} = \nabla V_m$. Use the constitutive relation between the magnetic flux density $\mathbf{B}$ and magnetic field

$$\mathbf{B} = \mu_0\left(\mathbf{H} + \mathbf{M}\right), \tag{14}$$

together with the following equation:

$$\nabla \cdot \mathbf{B} = 0. \tag{15}$$

Then V_m can be obtained from the following equation:

$$-\nabla \cdot \left(\mu_0 \nabla V_m - \mu_0 \mathbf{M}_0\right) = 0. \tag{16}$$

By introducing the Maxwell stress tensor to relate the magnetic field and mechanical field, a two-dimensional plane stress RVE for the MRE is developed in COMSOL Multiphysics to study its response under magnetic field. The magnetic vector potential $\mathbf{A}$ in the horizontal direction is input in the top and bottom boundaries. Consider

$$\mathbf{A}_z = \begin{cases} \mathbf{A}_{z,0}, & \text{top} \\ -\mathbf{A}_{z,0}, & \text{bottom}, \end{cases} \tag{17}$$

where $\mathbf{A}_{z,0}$ is the z-direction element of $\mathbf{A}_z$.

As shown in Figure 7, the black arrow is the Maxwell surface stress tensor. It also shows that the magnetic flux density under a horizontal direction in the 2D plane stress for the anisotropic MRE is larger than under a perpendicular direction. Obviously, this is caused by the directivity of the magnetic field.

5.3. Results and Discussions. Figure 8 shows the simple shear deformation under a magnetic field using PBC. Modeling analyses on the MREs are implemented to investigate the effect of magnetic field strength, the particle radius, and the distance between two adjacent particles on the shear modules.

As shown in Figures 9, 10, and 11, the initial shear modulus increases with increasing magnetic flux density and radius of particles and decreasing distance between two adjacent particles in a chain. The simulation results are in good agreement with theoretical results from the dipole model represented by (13). The magnetic field will cause the magnetic force and thus will result in compression of

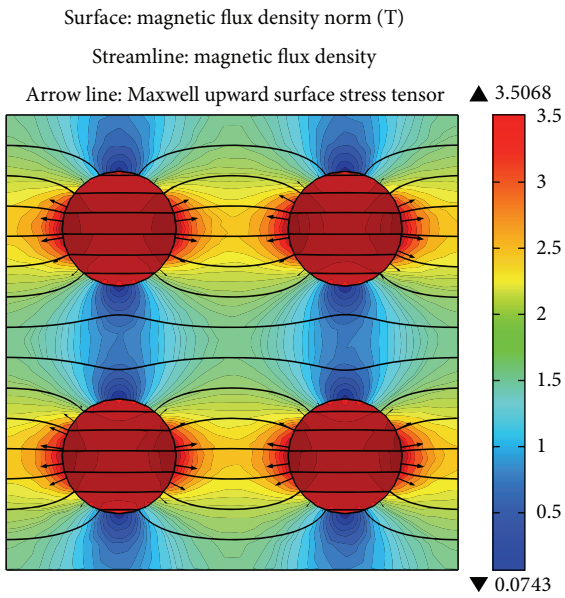

Figure 7: Magnet flux density in MRE.

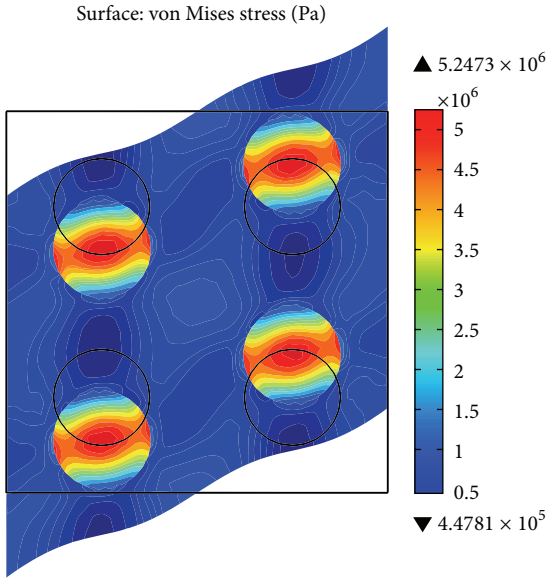

Figure 8: Shear deformation in MRE.

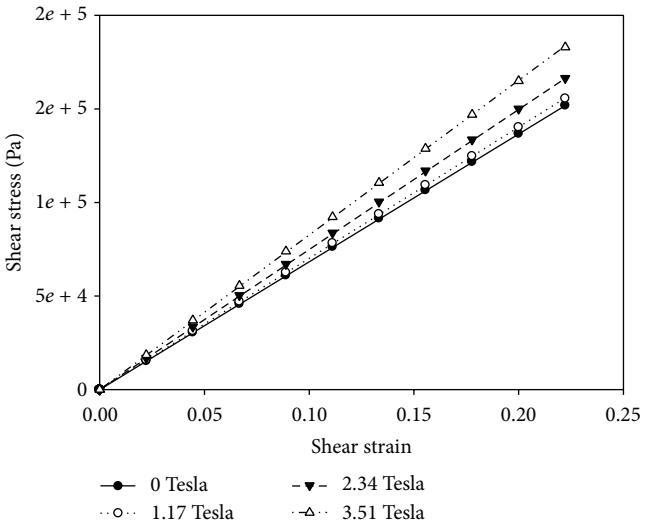

Figure 9: Different magnetic field strength.

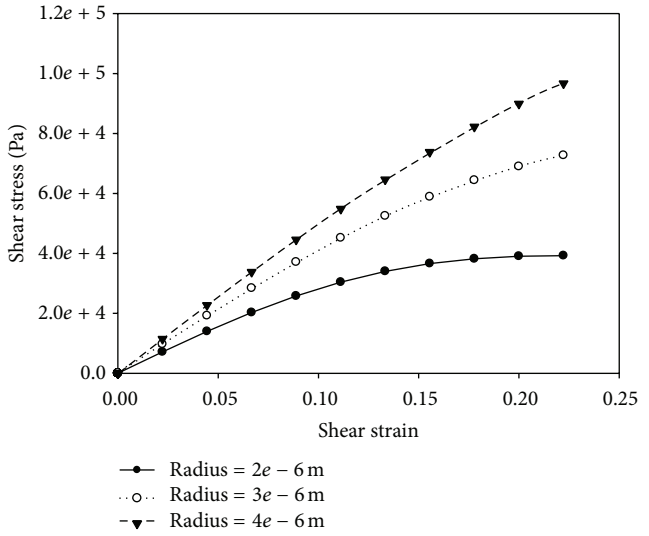

Figure 10: Different radius of particles.

the matrix (rubber), which is actually magnetic prestressed. This is explained by the fact the particles attract each other and thus increase the stiffness of material in some way. If a shear deformation is implemented, it must overcome the magnetic force in the direction of the magnetic field. So, the shear stress increases with the increase of magnetic flux density. For the same reason, the magnetic force and the shear stress increase with increasing radius of particles and decreasing distance between two adjacent particles.

6. Conclusion

In this paper, by using ABAQUS and COMSOL Multiphysics, magnetic-mechanical behaviors of MREs are investigated via FE simulations on RVEs with periodic boundary conditions being applied. An analysis of 3D RVE for the MRE without a magnetic field shows that the initial shear modulus of the MRE increases to nearly 1.56 times compared to that of the pure rubber acting as the matrix. A simple shear deformation of plane stress RVE using the Maxwell stress tensor is further implemented to characterize the properties of anisotropic MRE in the presence of a magnetic field. The numerical results show that an increase in initial shear modulus can be achieved when the intensity of magnetic field and radius of particles increase and the distance between two adjacent particles decreases. All the modeling results are in good agreement with theoretical results. Future works will be concentrated on the macro-/micromechanical properties of anisotropic MREs by using three-dimensional FEM.

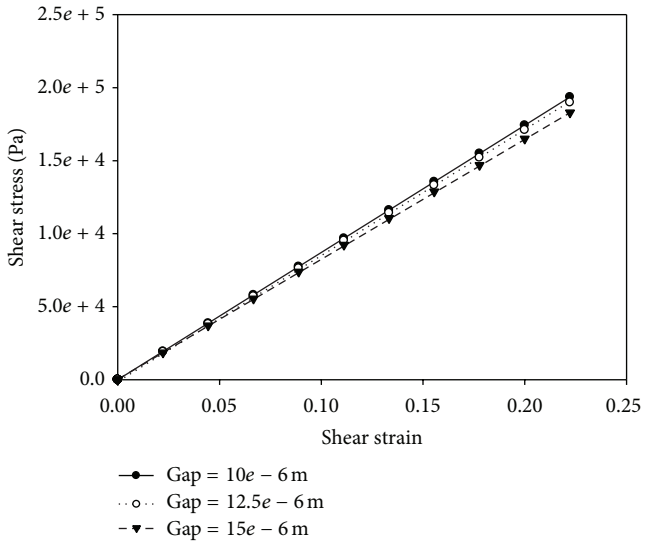

Figure 11: Different distance between two adjacent particles.

Conflict of Interests

The authors declare that there is no conflict of interests regarding the publication of this paper.

Acknowledgments

The supports from the National Natural Science Foundation of China (11172171 and 11272362) and Ph.D. Programs Foundation of Ministry of Education of China (20130073110054) are gratefully acknowledged.

References

[1] L. Borcea and O. Bruno, "On the magneto-elastic properties of elastomer-ferromagnet composites," *Journal of the Mechanics and Physics of Solids*, vol. 49, no. 12, pp. 2877–2919, 2001.

[2] T. A. Duenas and G. P. Carman, "Large magnetostrictive response of Terfenol-*D* resin composites (invited)," *Journal of Applied Physics*, vol. 87, no. 9, pp. 4696–4701, 2000.

[3] S. Jin, T. H. Tiefel, R. Wolfe, R. C. Sherwood, and J. J. Mottine Jr., "Optically transparent, electrically conductive composite medium," *Science*, vol. 255, no. 5043, pp. 446–448, 1992.

[4] L. Sandlund, M. Fahlander, T. Cedell, A. E. Clark, J. B. Restorff, and M. Wun-Fogle, "Magnetostriction, elastic moduli, and coupling factors of composite Terfenol-D," *Journal of Applied Physics*, vol. 75, no. 10, pp. 5656–5658, 1994.

[5] L. Ge, X. Gong, Y. Fan, and S. Xuan, "Preparation and mechanical properties of the magnetorheological elastomer based on natural rubber/rosin glycerin hybrid matrix," *Smart Materials and Structures*, vol. 22, Article ID 115029, 2013.

[6] W. Jiang, Z. Cao, R. Gu, X. Ye, C. Jiang, and X. Gong, "A simple route to synthesize $ZnFe_2O_4$ hollow spheres and their magnetorheological characteristics," *Smart Materials and Structures*, vol. 18, no. 12, Article ID 125013, 2009.

[7] J. Yang, X. Gong, L. Zong, C. Peng, and S. Xuan, "Silicon carbide-strengthened magnetorheological elastomer: preparation and mechanical property," *Polymer Engineering and Science*, 2013.

[8] W. Zhang, X. Gong, W. Jiang, and Y. Fan, "Investigation of the durability of anisotropic magnetorheological elastomers based on mixed rubber," *Smart Materials and Structures*, vol. 19, no. 8, Article ID 085008, 2010.

[9] A. Dorfmann and R. W. Ogden, "Magnetoelastic modelling of elastomers," *European Journal of Mechanics A: Solids*, vol. 22, no. 4, pp. 497–507, 2003.

[10] L. C. Davis, "Model of magnetorheological elastomers," *Journal of Applied Physics*, vol. 85, no. 6, pp. 3348–3351, 1999.

[11] M. R. Jolly, J. D. Carlson, B. C. Muñoz, and T. A. Bullions, "The magnetoviscoelastic response of elastomer composites consisting of ferrous particles embedded in a polymer matrix," *Journal of Intelligent Material Systems and Structures*, vol. 7, no. 6, pp. 613–622, 1996.

[12] Y. Shen, M. F. Golnaraghi, and G. R. Heppler, "Experimental research and modeling of magnetorheological elastomers," *Journal of Intelligent Material Systems and Structures*, vol. 15, no. 1, pp. 27–35, 2004.

[13] T. Shiga, A. Okada, and T. Kurauchi, "Magnetroviscoelastic behavior of composite gels," *Journal of Applied Polymer Science*, vol. 58, no. 4, pp. 787–792, 1995.

[14] H. H. Woodson and J. R. Melcher, *Electromechanical Dynamics*, Wiley, 1985.

[15] Y.-H. Pao, "Electromagnetic forces in deformable continua," in *Mechanics Today*, vol. 4 of *NSF-Supported Research*, pp. 209–305, Pergamon Press, New York, NY, USA, 1978.

[16] J. Mizia, K. Adamiak, A. R. Eastham, and G. E. Dawson, "Finite element force calculation: comparison of methods for electric machines," *IEEE Transactions on Magnetics*, vol. 24, no. 1, pp. 447–450, 1988.

[17] G. H. Jang, J. W. Yoon, N. Y. Park, and S. M. Jang, "Torque and unbalanced magnetic force in a rotational unsymmetric brushless DC motors," *IEEE Transactions on Magnetics*, vol. 32, no. 5, pp. 5157–5159, 1996.

[18] D. J. Griffiths and R. College, *Introduction to Electrodynamics*, Prentice Hall, Upper Saddle River, NJ, USA, 1999.

[19] A. Kovetz, *The Principles of Electromagnetic Theory*, Cambridge University Press, Cambridge, UK, 1990.

[20] O. B. Wilson, *Introduction to Theory and Design of Sonar Transducers*, Peninsula Publishing, Los Altos, Calif, USA, 1988.

[21] R. K. Wangsness, *Electromagnetic Fields*, vol. 1, Wiley-VCH, New York, NY, USA, 2nd edition, 1986.

[22] C. Chen, T. Lu, and N. Fleck, "Effect of imperfections on the yielding of two-dimensional foams," *Journal of the Mechanics and Physics of Solids*, vol. 47, no. 11, pp. 2235–2272, 1999.

[23] S. Demiray, W. Becker, and J. Hohe, "Analysis of two- and three-dimensional hyperelastic model foams under complex loading conditions," *Mechanics of Materials*, vol. 38, no. 11, pp. 985–1000, 2006.

[24] J. Hohe and W. Becker, "Geometrically nonlinear stress-strain behavior of hyperelastic solid foams," *Computational Materials Science*, vol. 28, no. 3-4, pp. 443–453, 2003.

[25] Z. Guo, X. Peng, and B. Moran, "Large deformation response of a hyperelastic fibre reinforced composite: theoretical model and numerical validation," *Composites A: Applied Science and Manufacturing*, vol. 38, no. 8, pp. 1842–1851, 2007.

[26] J. D. Eshelby, "The determination of the elastic field of an ellipsoidal inclusion, and related problems," *Proceedings of the Royal Society London A: Mathematical, Physical and Engineering Sciences*, vol. 241, pp. 376–396, 1957.

[27] T. Mori and K. Tanaka, "Average stress in matrix and average elastic energy of materials with misfitting inclusions," *Acta Metallurgica*, vol. 21, no. 5, pp. 571–574, 1973.

[28] S. Nemat-Nasser and M. Hori, "Micromechanics: overall properties of heterogeneous solids," in *Applied Mathematics and Mechanics*, Elsevier, Amsterdam, The Netherlands, 1993.

[29] Z. Guo, F. Caner, X. Peng, and B. Moran, "On constitutive modelling of porous neo-Hookean composites," *Journal of the Mechanics and Physics of Solids*, vol. 56, no. 6, pp. 2338–2357, 2008.

[30] Z. Guo, X. Shi, Y. Chen, H. Chen, X. Peng, and P. Harrison, "Mechanical modeling of incompressible particle-reinforced neo-Hookean composites based on numerical homogenization," *Mechanics of Materials*, vol. 70, pp. 1–17, 2014.

[31] J. S. Bergström and M. C. Boyce, "Mechanical behavior of particle filled elastomers," *Rubber Chemistry and Technology*, vol. 72, no. 4, pp. 633–656, 1999.

[32] M. C. Boyce and E. M. Arruda, "Constitutive models of rubber elasticity: a review," *Rubber Chemistry and Technology*, vol. 73, no. 3, pp. 504–523, 2000.

[33] A. N. Gent, *Engineering with Rubber: How to Design Rubber Components*, Hanser, 2001.

[34] R. Rosensweig, *Ferrohydrodyn Amics*, Cambridge University, New York, NY, USA, 1985.